Since January 2020 Elsevier has created a COVID-19 resource centre with free information in English and Mandarin on the novel coronavirus COVID-19. The COVID-19 resource centre is hosted on Elsevier Connect, the company's public news and information website.

Annals of Diagnostic Pathology 60 (2022) 151983

Contents lists available at ScienceDirect

Annals of Diagnostic Pathology

journal homepage: www.elsevier.com/locate/anndiagpath

Original Contribution

Histologic, viral, and molecular correlates of heart disease in fatal COVID-19

Louisa Mezache [a,1], Gerard J. Nuovo [b,c,*,1], David Suster [d], Esmerina Tili [e], Hamdy Awad [e], Przemysław B. Radwański [f], Rengasayee Veeraraghavan [a]

[a] Department of Biomedical Engineering, The Ohio State University, Columbus, OH, USA
[b] Ohio State University Comprehensive Cancer Center, Columbus, OH, USA
[c] GnomeDX, Powell, OH, USA
[d] Rutgers University Hospital Department of Pathology, Newark, NY, USA
[e] Ohio State University Medical Center, Columbus, OH, USA
[f] Division of Outcomes and Translational Sciences, The Ohio State University, Columbus, OH, USA

ARTICLE INFO

Keywords:
Myocardium
COVID-19
Myocarditis
Spike protein
Arrhythmia

ABSTRACT

Cardiac manifestations are common in severe COVID-19. This study compared the histologic, viral, and molecular findings in cardiac tissue in fatal COVID-19 (n = 11) and controls (n = 11). *In situ* hybridization (SARS-CoV2 RNA) and immunohistochemistry for viral proteins and the host response were quantified for the samples and compared with qRTPCR and Western blot data. Control hearts showed a high resident population of macrophages that had variable ACE2 expression. Cardiac ACE2 expression was 10× greater in the heart tissues of cases and controls with obesity or type II diabetes. Multifocal endothelial cell swelling and degeneration, perivascular edema plus microvascular thrombi were unique to the cases. SARS-CoV2 RNA and nucleocapsid protein were rarely detected *in situ* in any COVID-19 heart. However, in each case abundant SARS-CoV-2 spike protein was evident. Co-expression experiments showed that the spike protein localized mostly to the ACE2+ interstitial macrophages/pericytes that were activated as evidenced by increased IL6 and TNFα expression. Western blots confirmed the presence of the viral spike protein, but not the nucleocapsid protein, in the cardiac homogenates. The intercalated disc proteins connexin 43, the primary cardiac gap junction protein, and $Na_V1.5$, the predominant cardiac sodium channel, each showed marked lateral migration in the myocytes in the cases, which would increase the risk of reentrant arrhythmias. It is concluded that the viral spike protein, endocytosed by macrophages/pericytes, can induce a myocarditis with the possibility of conduction dysfunction due to abnormal localization of key intercalated disc proteins.

1. Introduction

The COVID-19 pandemic has, as of this writing, led to the infection of over 500 million people with more than 6 million deaths. Key risk factors for severe COVID-19 include obesity and diabetes mellitus that is independent of age which is important in the USA given that the obesity rate is 40.0% in the age group 20–39 and 21.2% among 12–19 year old's [1,2]. A major unresolved question in severe/fatal COVID-19 is whether the multi-organ failure typical of the disease state reflects infectious virus in these diverse organs, reportedly with the endothelial cells being a primary target, or is a consequence of the systemic cytokine storm and coagulopathy documented in the end-stage disease [3-11].

Cardiac disease is a well-documented and common problem in severe COVID-19 with rates reported from 2% in non ICU patients to 59% in non-survivors [6]. The latter finding is not surprising given that it has been reported that the SARS-CoV2 receptor, ACE2, is expressed in the heart in amounts greater than the lung [5-7] and may be evident in endothelial cells, macrophages, and pericytes. Importantly, obesity and diabetes have been associated with increased ACE2 expression in the heart along with the protease TMPRSS2 which may facilitate spike protein cell entry [5,6]. Other proteases involved in SARS-CoV2 spike protein entry into cells, such as furin, and cathepsin L, are strongly

* Corresponding author at: 1476 Manning Parkway, Powell, OH, USA.
E-mail address: nuovo.1@osu.edu (G.J. Nuovo).
[1] These two authors contributed equally to the work.

https://doi.org/10.1016/j.anndiagpath.2022.151983

Available online 29 May 2022

expressed in the heart [5,6]. The elevated ACE2 expression in the heart is not reduced by treatment with ACE inhibitors [5,10]. Pathologic changes reported in the heart in COVID-19 include cardiac nonocclusive microvascular thrombi in 80% of active cases and myocarditis in 33% [8]. Cardiac manifestations of severe COVID-19 include bradycardia, tachycardia, and arrhythmias [5,9].

With regards to the pathophysiology of cardiac disease in severe COVID-19, the results have been disparate. Several studies, using *in vitro* engineered heart tissues or human induced pluripotent stem cells have suggested that cardiomyocytes may be directly infected by SARS-CoV2 [12,13], another study suggested that the mechanism was a diffuse infectious endothelialitis [14], whereas a recent study indicated marked macrophage activation in the myocardium in severe COVID-19. Other studies have either not detected infectious virus in the heart, or suggested that the cardiac damage may reflect the systemic cytokine storm and coagulopathy that is well documented in the end-stage disease [3,4,8,11].

The purpose of this study was to examine cardiac tissues from 11 people who died of COVID-19 and compare the molecular/histologic/viral findings in a blinded fashion to 11 pre-COVID controls to better define the mechanism(s) whereby SARS-CoV2 can induce cardiac disease. The histologic analyses should assist the diagnostic pathologist when reviewing heart tissue to be able to ascertain COVID-19 related changes under the microscope.

2. Materials and methods

2.1. COVID-19 autopsies and controls

Complete autopsy material (except in 1 case where the CNS was not removed) was available from 11 people who died of COVID-19. They ranged in age from 36 to 92 (mean 71; six men and five women). The heart tissues from eleven aged matched controls from people who died prior to 2016 served as negative controls where, for six people, the cardiac tissue was described as unremarkable and the other five had hypertensive cardiomegaly including three with scars from myocardial infarctions from 12 to 24 months prior to death. Salient clinical information included that 9/11 cases had pre-existing cardiac disease defined as cardiomegaly from hypertensive chronic heart disease. Seven of the cases had obesity, six had type II diabetes, five had coronary artery disease, one had alcohol-related myopathy, and one had chronic atrial fibrillation. Six of the control hearts came from people listed with obesity and/or type II diabetes and the three pre-COVID old myocardial infarct cases each had coronary artery disease. For qRTPCR and Western blot analyzes, in selected cases five ten micron paraffin ribbons were placed in sterile eppendorf tubes, the paraffin removed, and the RNA or protein extracted with the appropriate Qiagen kit as per the manufacturer's recommendations.

2.2. Immunohistochemistry

Immunohistochemistry was done as previously reported [15-17]. In brief, optimal conditions for each antibody were determined by testing various dilutions and pretreatment conditions. The SARS-CoV2 specific antibodies were from ProSci (Poway, CA) [15-17].

In brief, the immunohistochemistry protocol used the Leica Bond Max automated platform. Both the Fast red (DS 9820) and the DAB (DS 9800) detection kits from Leica Biosystems (Buffalo Grove, IL) were used and gave equivalent results. The host response was interrogated with antibodies against activated caspase 3, IL6, TNFα, complement component 6 as well as ACE2. Cell specific markers included CD31 (endothelial cells), smooth muscle actin (SMA) (pericytes) and a panel of proteins for macrophages that included CD68, CD11b, CD163, and CD206. The HRP conjugate from Enzo Life Sciences (Farmingdale, New York, USA) was used in cases in place of the equivalent reagent from Leica in the DAB kit as this has been shown to reduce background for some primary antibodies [15-17].

2.3. In situ hybridization

Detection of SARS-CoV-2 RNA was done using the ACD RNAscope (Newark, California, USA) probe (Cat No. 848561-C3) using the manufacturers recommended protocol as previously published [10-12].

2.4. Co-expression and statistical analyses

Co-expression analyses were done using the Nuance/InForm system whereby each chromogenic signal is separated, converted to a fluorescence-based signal, then mixed to determine what percentage of cells were expressing the two proteins of interest as previously described [13-15]. The number of positive cells/200× field was counted with the InForm software or manually in 10 fields/tissue. Statistical analysis was done using the InStat Statistical Analysis Software (version 3.36) and a paired *t*-test (also referred to as a "repeated measure *t*-test"). The null hypothesis was rejected if the significance level was below 5%.

2.5. qRTPCR and Western blot analyses

For qRTPCR, each sample was reverse transcribed and pre-amplified in a Specific Target Amplification (COVID19 N1, N2, and Human RNase P targets) for CoVid19 detection. The reverse transcribed and pre-amplified cDNA was diluted and then detected by qPCR on the Fluidigm microfluidics platform using the CDC developed assays for CoVid19 N1, N2, and Human Rnase P.

Western blot analyses were done using identical amounts of protein extracted from the formalin fixed paraffin embedded tissues using Mini-PROTEA TGX premade gels according to the manufacturer's recommendations (BioRad). Unfixed swabs from the nasopharynx either positive or negative for SARS-CoV2 by qRTPCR as well as pre-COVID-19 lung/COVID-19 lung fixed in formalin served as the controls. Band detection was *via* the Enzo Life Sciences Western blot kit as per the manufacturer's recommendations.

3. Results

3.1. Clinical/pathologic correlation

Eleven autopsies from people who died of COVID-19 were studied with eleven age-matched controls. The cases ranged in age from 36 to 92 (mean 74; six men and five women). The negative controls were from people who died prior to 2016 and included six histologically normal hearts and five hearts from people with hypertensive cardiomegaly that showed focal fibrosis including three with old (>6 month) myocardial infarcts. Salient clinical information included that 9/11 cases had pre-existing cardiac disease (each had cardiomegaly from hypertensive chronic heart disease, though none were listed to have congestive heart failure prior to COVID-19, six were obese and five had type II diabetes). Five of the control cases were from people with diabetes and/or obesity. The cause of death in each case was listed as severe viral induced bronchopneumonia and in six cases DIC/multiorgan failure was documented. Five of the eleven cases had atrial fibrillation noted during their COVID-19 related disease course.

3.2. Histologic changes

The hematoxylin and eosin stains were reviewed blinded to the clinical information. The cases showed three histologic changes: 1) scattered microvessels with enlarged, atypical endothelial cells, 2) microthrombi with perivascular extravasation of red blood cells, and 3) perivascular edema at times associated with perivascular collections of mononuclear cells (Fig. 1). The findings were consistent among the 11 cases and not seen in the controls with a mean of 1.9 microvessels/100×

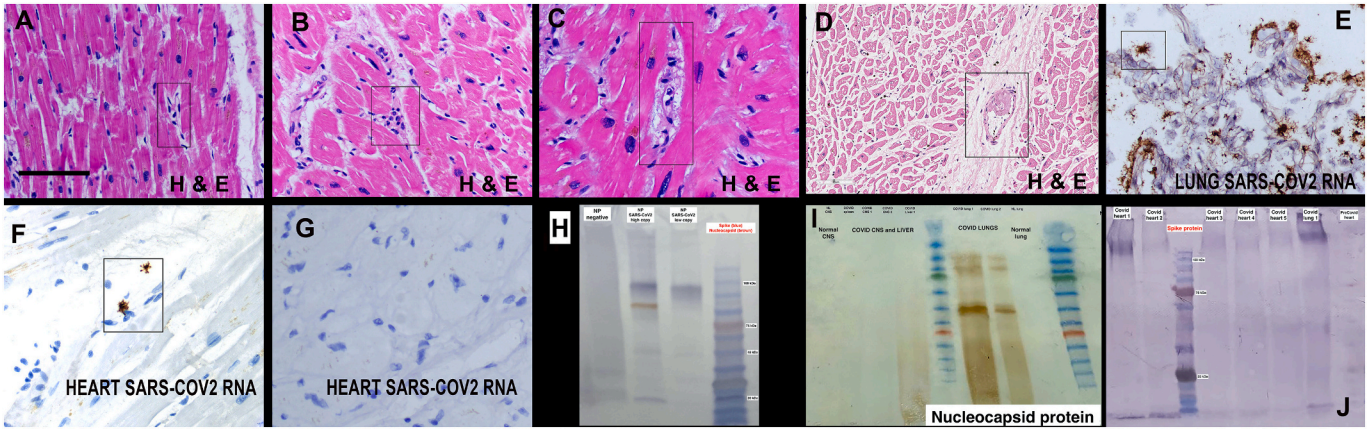

Fig. 1. Histologic findings and detection of viral RNA/proteins in the heart in fatal COVID-19. Panels A-D show the histologic findings in the heart unique to the COVID-19 cases. Note the enlarged, atypical endothelial cells (A, C), perivascular prominence of mononuclear cells (B), perivascular edema (C) and microvascular thrombi (D) (rectangles). Panel E shows the high copy number SARS-CoV2 RNA in the lung; note that the heart from the same person showed only two viral RNA positive cell in the entire section (panel F, rectangle); note the stellate type shape typical of macrophages. More commonly, SARS-CoV2 RNA was not evident in the entire section (panel G). Panel H shows the controls for the Western blot from proteins extracted either from the nasopharynx with no evident of SARS-CoV2 or a positive result by qRTPCR. Note that when tested for the viral spike protein a smaller band alone with the larger band may be evident. Also note the dual detection of spike protein (blue bands) and nucleocapsid protein (brown band) in the same blot. Panel I illustrates that the nucleocapsid protein in only evident in the COVID-19 lung samples and nasopharynx, and not in any other organs tested. Most of the COVID-19 heart samples showed a band when analyzed for the viral spike protein (panel J). The scale bars in each figure represent 200 μm. (For interpretation of the references to colour in this figure legend, the reader is referred to the web version of this article.)

field demonstrating at least one of these abnormal microvascular findings.

3.3. qRTPCR/in situ hybridization and Western blot analyses

The distribution of SARS-CoV2 RNA and protein were next assessed in the cardiac samples. The lung tissues from four of the cases were used as the positive controls as each were assessed to have high viral copy load by qRTPCR. The corresponding heart tissues from these viral positive lung samples were each negative by qRTPCR for viral RNA (data not shown). Each of the 22 cardiac samples were tested by *in situ* hybridization and scored in a blinded fashion. None of the controls were positive. The four lung tissues from the fatal COVID-19 cases each showed high copy RNA by *in situ* hybridization with a mean of >25+ cells/200× field in each (Fig. 1). Three of the eleven COVID-19 heart cases were positive for viral RNA. However, as seen in Fig. 1, these viral RNA-positive cases showed rare positive cells, that ranged from 1 to 4 for the entire 1–1.5 cm of tissue. Thus, viral RNA was either not detected (8 cases) or detected in very few cells (3 cases) in the heart, despite the high viral load evident in the corresponding lung tissue (Fig. 1).

Western blots were performed from the proteins extracted from the formalin-fixed, paraffin embedded tissues for the nucleocapsid protein, as well as for the viral spike and envelope proteins. Proteins extracted from unfixed nasopharyngeal swabs positive and negative for SARS-CoV2 was used to validate the assay (Fig. 1). Normal skin biopsies divided into unfixed *versus* formalin-fixed/paraffin embedded were used to document that the expected sized bands for type I/III collagen were detected in both samples, although there was a 50% reduction in signal intensity in the latter (data not shown).

Proteins extracted from COVID-19 lung and heart formalin fixed, paraffin embedded tissues were then tested for viral spike subunit 1, nucleocapsid, and envelope proteins. The samples positive for nucleocapsid, and envelope proteins gave discrete bands in the Western blots (Fig. 1). However, the samples positive for the viral spike protein usually showed multiple bands that included the expected sizes of 180 (full length) and 90 KDa (cleaved upon viral entry), as well as many other bands as small as 17 KDa (Fig. 1). Interestingly, only the COVID-19 lung and nasopharyngeal samples showed a signal for the nucleocapsid protein (Fig. 1). Specifically, 0/11 cardiac cases were positive for the nucleocapsid protein whereas 7/11 were positive for the viral spike (Fig. 1) and envelope proteins (data not shown).

3.4. Immunohistochemistry for viral proteins

The Western blot/qRTPCR data suggested that not the infectious virus but rather the spike protein in combination with other viral membrane proteins may be concentrating in the heart. Thus, the 20 heart samples were tested for the nucleocapsid, spike, matrix, and envelope proteins by immunohistochemistry blinded to the clinical information.

The viral nucleocapsid protein was detected in 2/11 of the cardiac samples, which included two cases that were also positive for the viral RNA, in none of the controls, and in 5/5 of the corresponding lung tissues. Representative data is provided in Fig. 2. The viral spike protein was detected in 11/11 of the COVID-19 hearts, none of the controls, and 5/5 of the corresponding lung samples (Fig. 2). Note the equivalent distribution of viral spike, envelope, and matrix proteins which, as expected based on this pattern, showed strong co-localization (data not shown); no signal was evident in the controls (Fig. 2). The mean number of spike positive cells/200× field was high (2.3 (0.7)). Note that the viral capsid proteins typically localized around the microvessels which is the same pattern seen for the macrophage marker CD68 and the viral spike receptor ACE2 (Fig. 2). Indeed, co-expression data documented that many of the cells which contained the viral spike protein also expressed CD68 (Fig. 2).

3.5. Immunohistochemistry for ACE2, cardiac macrophage and pericyte markers

The 11 cases and controls were next interrogated by immunohistochemistry for the immune cell markers that populate this area including T cells (CD3), B cells (CD20), and macrophages (CD68, CD11b, CD163, and CD206) blinded to the clinical information.

There were very few T or B cells in either the control or the COVID-19 hearts. The numbers of each cell type expressed as percentage of cells (mean/SEM) were as follows: **CD3** (normal, 0.2/0.1 and COVID-19, 0.2/0.1; **CD20** (normal 0 and COVID-19, 0.1/01.). The macrophage quantification data demonstrated two points: 1) there is an abundant

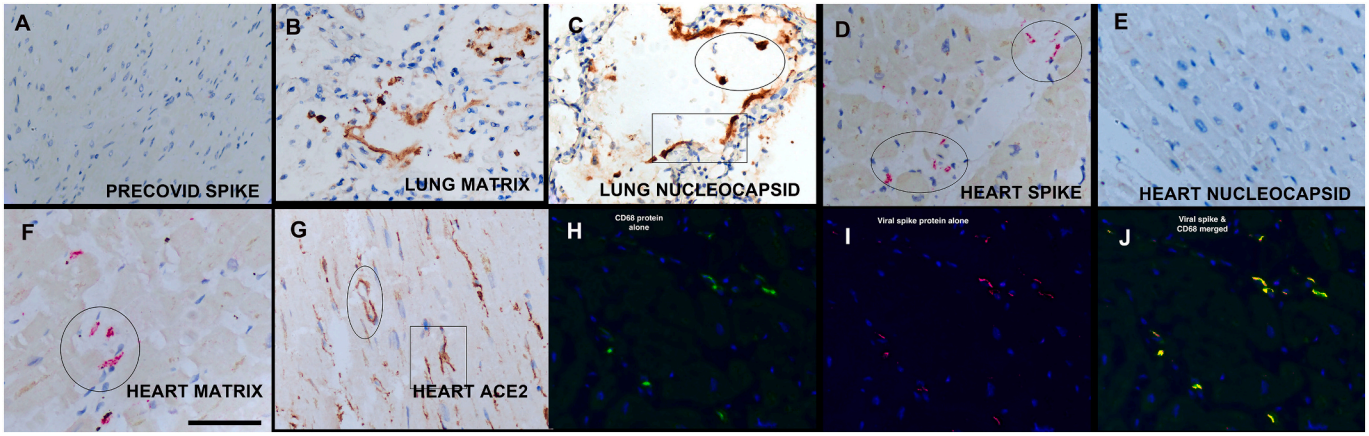

Fig. 2. *In situ* detection of viral proteins in the heart in fatal COVID-19.
Note the absence of the viral spike protein in the pre-COVID negative controls (panel A) and the intense signal in equivalent distributions for the viral matrix and nucleocapsid protein in the lung (panels B and C). Each of the COVID-19 heart samples showed a signal for the spike (panel D), matrix (panel F) and envelope proteins (not shown) but none showed a diffuse signal for the nucleocapsid protein (panel E); note the perivascular distribution of the signal which was the same pattern evident for the viral receptor ACE2 (panel G). Note that the ACE2 signal is seen both in the perimeter of the microvessels (G, oval) and in stellate shaped cells with the morphology of macrophages (rectangle). Panels H-J show co-expression of CD68 (isolated in H), the viral spike protein (isolated in I) and the merged image that documents that many of the cells that contain the viral spike protein are CD68+ macrophages (panel J).

endogenous population of macrophages as measured with four different markers in the normal heart and 2) although there was an upward trend in the cells with the macrophage markers in the COVID-19 heart, the increases did not reach statistical significance. The specific data (presented as the % of positive cells, mean/SD) was as follows: **CD11b** (normal, 2.0/1.0 and COVID-19, 2.9/1.1), **CD163** (normal, 10.9/2.2 and COVID-19, 13.9/4.0), **CD206** (normal, 1.2/0.5 and COVID-19, 1.6/0.8), and **CD68** (normal, 10.5/4.1 and COVID-19, 12.8/4.7). Representative data for several of the macrophage markers are provided in Fig. 3. Note that the macrophage markers often intertwined with the walls of the microvessels. Co-expression analyses showed that these different macrophage markers did show co-localization with the endothelial marker CD31 (data not shown). Similarly, the pericyte marker SMA (smooth muscle actin) likewise showed a strong signal around the microvessels. As seen in Fig. 3, the SMA signal often had a beaded appearance and it also showed co-expression with CD31 (data not shown), indicating possible direct communication between the pericytes and endothelia.

Next, immunohistochemistry for ACE2 was done on the 22 heart samples. As seen in Fig. 3, ACE2 also showed a perivascular/interstitial pattern. There was a significant increase in the number of ACE2+ cells in the COVID-19 cases (9.6/1.9) *versus* the six normal hearts from non-obese people (mean/SE) (1.0/0.5), $p < 0.001$. However, the data was similar when examining the six obese people who died of COVID-19 (% of ACE2+ cells in the myocardium = 11.4/4.4) and the five obese people in the controls who had old myocardial infarctions (8.1/3.8). The ACE2 + cells showed strong co-expression with the macrophage and pericyte markers (Fig. 3).

3.6. Immunohistochemistry for host response to virus

Immunohistochemistry was done for caspase 3, IL6, and TNFα as each has been associated with the cytokine storm of fatal COVID-19. The controls showed no *in situ* expression of IL6 or TNFα and rare cells positive for caspase 3 (1–2 per 1 cm section) (Fig. 4). Each cytokine was detected in the 11 COVID-19 heart samples. As seen in Fig. 4, the cells that expressed TNFα, IL6, and caspase 3 localized to the perivascular zone of the myocardial interstitium. Co-expression documented that the

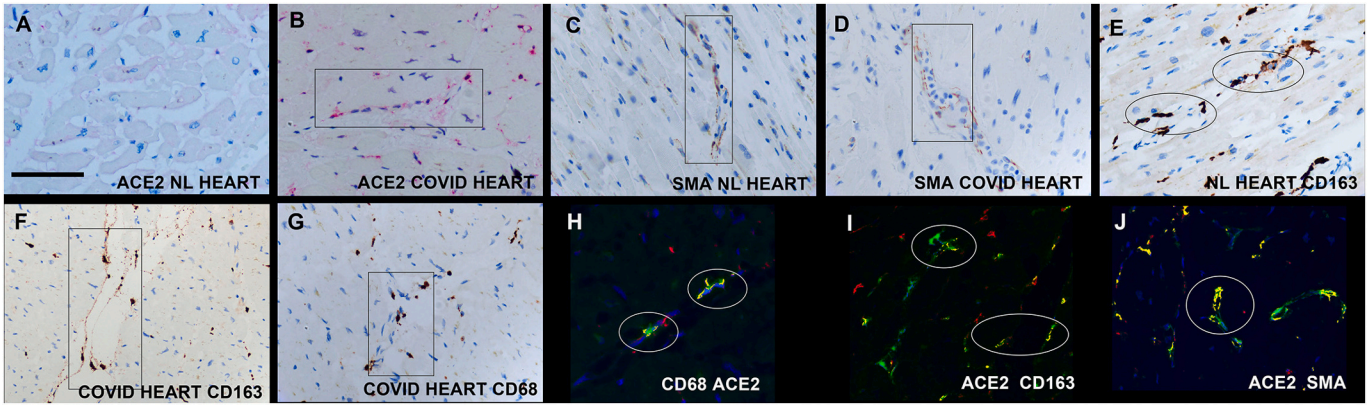

Fig. 3. Macrophages, pericytes, and ACE2 in the heart in fatal COVID-19.
Panel A shows the sparse detection of ACE2 protein in the normal heart compared to the high expression in the COVID-19 heart in a person who had type II diabetes and obesity (panel B); note the perivascular distribution of ACE2 (rectangle). Panels C and D show the perivascular distribution of the pericyte marker SMA in the normal (C) and COVID heart (D) (rectangles). Panels E and F show the perivascular distribution of the macrophage marker CD163 in the normal (E) and COVID heart (F) as well as the macrophage marker CD68 (G); note in panel F how the macrophages entwine the microvessel (rectangle). Panels H-J show co-expression experiments where co-localization is indicted by fluorescent yellow; note that ACE2 is found in CD68+ macrophages (panel H) as well as CD163+ macrophages (panel I) and the pericyte marker SMA (panel J). (For interpretation of the references to colour in this figure legend, the reader is referred to the web version of this article.)

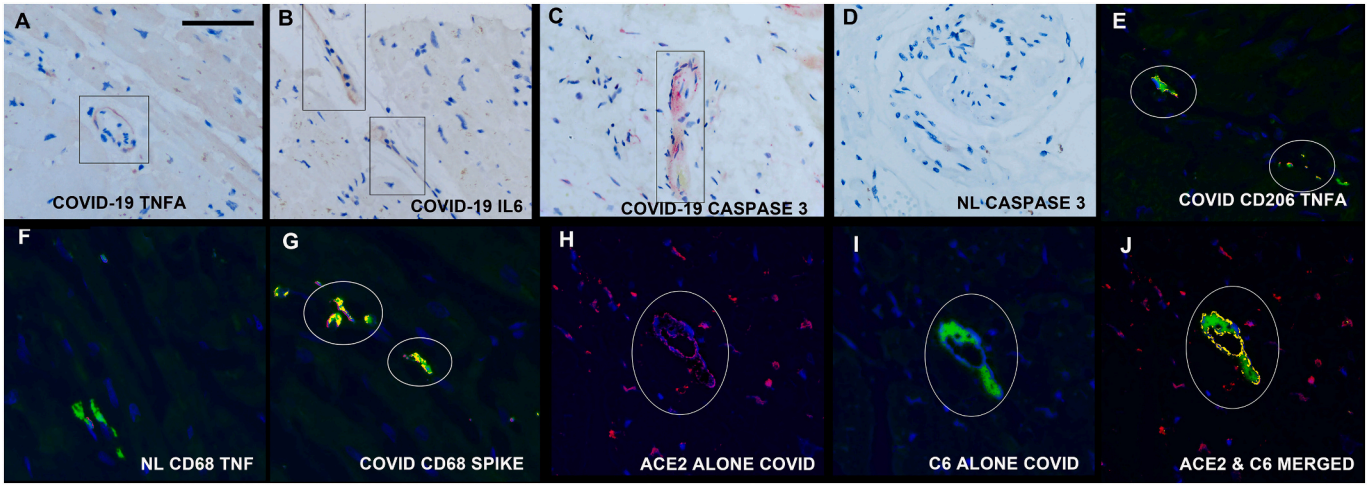

Fig. 4. Host response in the heart in fatal COVID-19. TNFα. Panels A-C show serial sections of the heart in a fatal COVID-19 case where TNFα, IL6, and caspase 3, respectively, were evident in the same perivascular distribution (rectangles). Panel D is a negative control (caspase 3 in a normal preCOVID heart). Co-expression analyses, where co-localization of two targets (fluorescent red and green) is seen as fluorescent yellow indicated that the TNFα was present in macrophages (panel E, CD206) and that the macrophages contained most of the spike protein (panel G); panel F is a negative control of CD68 (green) and TNFα (red) in a normal pre-COVID heart. Panels H-J show the individual images of ACE 2 (red, panel H), complement component 6 (panel I) and the merged image in panel J, demonstrating that some of the hypercoagulability evident in the heart was induced *in situ*. (For interpretation of the references to colour in this figure legend, the reader is referred to the web version of this article.)

cytokines were expressed in macrophages and pericytes and that these cell types also contained the viral spike protein (Fig. 4).

Since complement activation is also associated with severe COVID-19, the heart tissues were tested for complement component 6. This protein was increased and showed a perivascular pattern around the microvessels and was not evident in the controls. Note in Fig. 5 that complement 6 localized to ACE2+ cells.

3.7. Intercalated disc proteins in COVID-19

The *in situ* distribution of three key intercalated disc proteins, N-cadherin, connexin 43 (Cx43), and $Na_V1.5$ was next examined. As seen in Fig. 5, each of these three proteins showed a sharp demarcation along a perpendicular plane in the myocyte in the control, histologically normal hearts. The N cadherin signal maintained this pattern in each of the COVID-19 heart samples. However, both Cx43 and $Na_V1.5$ showed marked lateralization away from the intercalated disc towards the lateral myocyte cell membrane in each of the COVID-19 heart samples (Fig. 5). Although the patterns varied among the different COVID-19 heart samples with varying maintenance of the intercalated disc localization, all COVID-19 cases showed at least 1/3 of the signal lateralizing to the periphery of the myocyte. This pattern was then compared to the pre-COVID-19 hearts where there was pre-existing heart disease including hypertensive cardiomegaly, and/or chronic myocardial

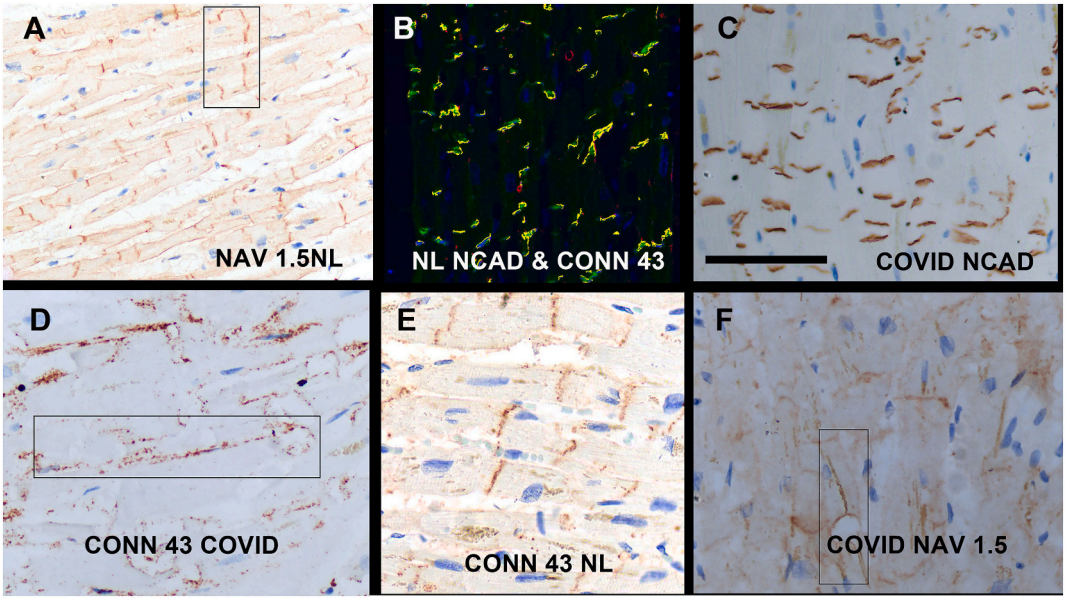

Fig. 5. Alterations in key intercalated disc proteins in the heart in fatal COVID-19. Panels A and B show the distribution of $Na_V1.5$ (panel A) and N cadherin plus connexin-43 (co-localization with N cadherin fluorescent green and connexin-43 red) in the normal pre-COVID heart; note the strong localization to the intercalated disc region that is perpendicular to the long axis of the myocyte. Each of the heart tissues from fatal COVID-19 cases showed the baseline pattern for N cadherin (panel C) but each showed substantial marked migration of the Cx43 (panel D with panel E being a normal pre-COVID control) and $Na_V1.5$ signals (panel F) to the lateral border of the myocyte (rectangles). (For interpretation of the references to colour in this figure legend, the reader is referred to the web version of this article.)

infarction (5 cases). As with the COVID-19 cases, none of the cases had a history of congestive heart failure. There was strong co-localization of N-cadherin and connexin-43 in each of the pre-COVID-19 controls with pre-existing heart disease, However, lateral migration of Na_v 1.5 were seen in 3/5 of the pre-COVID-19 controls with pre-existing cardiomegaly from hypertensive heart disease. Each of the six pre-COVID-19 controls without pre-existing hypertensive cardiomegaly, including cases with diabetes type II, showed a normal pattern of connexin 43 and Nav-1.5 (data not shown).

4. Discussion

The focus of this study was to address a critical question on the common problem of cardiac disease in severe COVID-19: does the pathophysiology of the disease represent direct viral infection of the heart or the systemic manifestations of the cytokine storm and hypercoagulable propensity of the end stage disease state? This study strongly suggests that direct infection of the myocardium by SARS-CoV2 is not a factor in the pathophysiology of cardiac dysfunction. Although it is likely that the systemic manifestations of severe COVID-19 directly impact cardiac function, the primary and novel finding of this study is that there is substantial *in situ* expression of cytokines and complement activation in the heart secondary to endocytosis of circulating spike proteins by cardiac interstitial macrophages and pericytes which, in turn, induces a myocarditis. This is consistent with a recent study that showed that the spike protein *per se* can be cytotoxic to the heart and indicated that the viral protein can enter pericytes *via* the CD147 receptor and bypass ACE 2 [18].

This study, as have others, emphasized that the heart has a large endogenous population of macrophages and pericytes that are in direct contact with the endothelial cells of microvessels which may offer a defense mechanism to rapidly deal with systemically borne pathogens. A key finding of this study, documented by other investigators, is that these cells, as well as endothelial cells, strongly express ACE2 in the cardiac tissues [5-7,10]. Critically, diseases such as obesity and type II diabetes markedly increase ACE2 expression in these cells in the heart, as noted in this study, which would predispose these people to increased cardiac damage after infection with SARS-CoV2 [5-7,10]. The source of the endogenous spike protein in severe COVID-19 would likely be the extremely high copy viral load seen in the lungs of these patients. The virus in the lung induces a microangiopathy that causes viral degeneration and is a logical source of viral spike proteins entering the circulation and docking in organs with a high perivascular based ACE2 population, such as the heart [15]. Preliminary data suggests that the viral spike protein, alone with the matrix and envelope proteins, are carried by macrophages in the circulation (Nuovo GJ and Tili, E, unpublished observations). This could explain the many studies which have shown that the viral spike protein *per se*, or more accurately the S1 subunit of the spike protein, which has the RBD sequence for ACE2 binding, can demonstrate cytotoxic effects [19-25]. Viral RNA detection in this study was done by qRTPCR and an ultrasensitive *in situ* hybridization assay which has been documented to have equivalent sensitivity to PCR-based assays. Viral protein detection was likewise done by two orthogonal methods – Western blot and immunohistochemistry. The Western blot assay on the COVID-19 heart homogenates did show decreased sensitivity albeit with good specificity since formalin-fixed, paraffin-embedded tissues were used. The extensive co-localization data supports the hypothesis that the spike protein *per se* concentrates in cells in the interstitium of the heart, likely through migrating macrophages and pericytes, which are activated and express pro-inflammatory cytokines.

Notably, hearts from fatal COVID-19 cases demonstrated substantial lateralization of the gap junction protein connexin 43 and the cardiac sodium channel $Na_V1.5$. Loss of these proteins from the intercalated disks, sites of electromechanical contact between adjacent myocytes, has been demonstrated to impair electrical impulse propagation and thereby, promote reentrant arrhythmias in multiple cardiac pathologies [26-31]. Indeed, the combined impairment of excitability due to mislocalization/loss of $Na_V1.5$ and cell-to-cell coupling due to lateralization/loss of connexin 43 gap junctions is well established as posing a high risk of reentrant arrhythmias [26-31]. While the mechanisms underlying such remodeling of connexin 43 and $Na_V1.5$ have yet to be fully clarified, some clues may be gleaned from our recent demonstration that clinically relevant levels of inflammation dynamically ($\leq$1 h) induced swelling and translocation of $Na_V1.5$ from intercalated disk nanodomains in murine hearts, slowing impulse propagation and promoting arrhythmias [32]. These data support the hypothesis that inflammatory responses elicited by the viral spike protein could underlie lateralization of key intercalated disk proteins, thereby promoting reentrant arrhythmias in severe COVID-19.

Declaration of competing interest

The authors have no conflicts of interest to disclose.

Acknowledgments

The authors greatly appreciate the help of Dr. Margaret Nuovo with the photomicroscopy, Dr. Saul Suster who provided many of the samples, Dr. Cynthia Magro who provided samples and advice/comments and Ms. Eva Matys who performed most of the Western blots.

References

[1] Fryar CD, Carroll MD, Afful J. Prevalence of overweight, obesity, and severe obesity among children and adolescents aged 2–19 years: United States, 1963–1965 through 2017–2018. NCHS Health E-Stats; 2020.
[2] Hales CM, Carroll MD, Fryar CD, Ogden CL. Prevalence of obesity and severe obesity among adults: United States, 2017–2018. In: NCHS Data Brief, no 360. Hyattsville, MD: National Center for Health Statistics; 2020.
[3] Zhang Y, Geng X, Tan Y, et al. New understanding of the damage of SARS-CoV-2 infection outside the respiratory system. Biomed Pharmacother 2020;127:110195. https://doi.org/10.1016/j.biopha.2020.110195.
[4] Li H, Liu L, Zhang D. SARS-CoV-2 and viral sepsis: observations and hypotheses. Lancet 2020;395(10235):1517–20. https://doi.org/10.1016/S0140-6736.
[5] Herman-Edelstein M, Guetta T, Barnea A, Waldman M, Ben-Dor N, Barak Y, Kornowski R, Arad M, Hochhauser E, Aravot D. Expression of the SARS-CoV-2 receptor ACE2 in human heart is associated with uncontrolled diabetes, obesity, and activation of the renin angiotensin system. Cardiovasc Diabetol 2021;20(1):90. 27).
[6] Liu H, Gai S, Wang X, Zeng J, Sun C, Zhao Y, Zheng Z. Single-cell analysis of SARS-CoV-2 receptor ACE2 and spike protein priming expression of proteases in the human heart. Cardiovasc Res 2020;116(10):1733–41. 01.
[7] Chen L, Li X, Chen M, Feng Y, Xiong C. The ACE2 expression in human heart indicates new potential mechanism of heart injury among patients infected with SARS-CoV-2. Cardiovasc Res 2020;116(6):1097–100. 01.
[8] Bois MC, Boire NA, Layman AJ, Aubry MC, Alexander MP, Roden AC, Hagen CE, Quinton RA, Larsen C, Erben Y, Majumdar R, Jenkins SM, Kipp BR, Lin PT, Maleszewski JJ. COVID-19-associated nonocclusive fibrin microthrombi in the heart. Circulation 2021;143(3):230–43. 19.
[9] Ho JS, Tambyah PA, Ho AF, Chan MY, Sia CH. Effect of coronavirus infection on the human heart: a scoping review. Eur J Prev Cardiol 2020;27(11):1136–48. 07.
[10] Chirinos JA, Cohen JB, Zhao L, Hanff T, Sweitzer N, Fang J, Corrales-Medina V, Anmar R, Morley M, Zamani P, Bhattacharya P, Brandimarto J, Jia Y, Basso MD, Wang Z, Ebert C, Ramirez-Valle F, Schafer PH, Seiffert D, Gordon DA, Cappola T. Clinical and proteomic correlates of plasma ACE2 (angiotensin-converting enzyme 2) in human heart failure. Hypertension 2020;76(5):1526–36. 11.
[11] Delorey TM, Ziegler CGK, Heimberg G, et al. COVID-19 tissue atlases reveal SARS-CoV-2 pathology and cellular targets. Nature 2021;595(7865):107–13. 07.
[12] Bailey AL, Dmytrenko O, Greenberg L, Bredemeyer AL, Ma P, Liu J, Penna V, Winkler ES, Sviben S, Brooks E, Nair AP, Heck KA, Rali AS, Simpson L, Saririan M, Hobohm D, Stump WT, Fitzpatrick JA, Xie X, Zhang X, Shi PY, Hinson JT, Gi WT, Schmidt C, Leuschner F, Lin CY, Diamond MS, Greenberg MJ, Lavine KJ. SARS-CoV-2 infects human engineered heart tissues and models COVID- 19 myocarditis. JACC Basic Transl Sci 2021 Apr;6(4):331–45.
[13] Perez-Bermejo JA, Kang S, Rockwood SJ, Simoneau CR, Joy DA, Silva AC, Ramadoss GN, Flanigan WR, Fozouni P, Li H, Chen PY, Nakamura K, Whitman JD, Hanson PJ, BM McManus, Ott M, Conklin BR, TC McDevitt. SARS-CoV-2 infection of human iPSC-derived cardiac cells reflects cytopathic features in hearts of patients with COVID-19. Sci Transl Med 2021;13(590). 21.
[14] Varga Z, Flammer AJ, Steiger P, Haberecker M, Andermatt R, Zinkernagel A, Mehra M, Schuepbach R, Ruschitzha F, Moch H. Endothelial cell infection and

endotheliitis in COVID-19. https://marlin-prod.literatumonline.com/pb-assets/Lancet/pdfs/S0140673620309375.pdf. 21.
[15] Magro C, Mulvey JJ, Berlin D, Nuovo G, Salvatore S, Harp J, Baxter-Stoltzfus A, Laurence J. Complement associated microvascular injury and thrombosis in the pathogenesis of severe COVID-19 infection: a report of five cases. Transl Res 2020; 220:1–13. 06.
[16] Nuovo GJ, Magro C, Mikhail A. Cytologic and molecular correlates of SARS-CoV-2 infection of the nasopharynx. Ann Diagn Pathol 2020 Oct;48:151565.
[17] Nuovo GJ, Magro C, Shaffer T, Awad H, Suster D, Mikhail S, He B, Michaille JJ, Liechty B, Tili E. Endothelial cell damage is the central part of COVID-19 and a mouse model induced by injection of the S1 subunit of the spike protein. Ann Diagn Pathol 2021 Apr;51:151682.
[18] Avolio E, Carrabba M, Milligan R, Kavanagh Williamson M, Beltrami AP, Gupta K, Elvers KT, Gamez M, Foster RR, Gillespie K, Hamilton F, Arnold D, Berger I, Davidson AD, Hill D, Caputo M, Madeddu P. The SARS-CoV-2 Spike protein disrupts human cardiac pericytes function through CD147 receptor-mediated signalling: a potential non-infective mechanism of COVID-19 microvascular disease. Clin Sci (Lond) 2021 Dec 22;135(24):2667–89. https://doi.org/10.1042/CS20210735. PMID: 34807265; PMCID: PMC8674568.
[19] Ogata AF, Cheng CA, Desjardins M, Senussi Y, Sherman AC, Powell M, Novack L, Von S, Li X, Baden LR, Walt DR. Circulating severe acute respiratory syndrome coronavirus 2 (SARS-CoV-2) vaccine antigen detected in the plasma of mRNA-1273 vaccine recipients. Clin Infect Dis 2022 Mar 1;74(4):715–8. https://doi.org/10.1093/cid/ciab465. PMID: 34015087; PMCID: PMC8241425.
[20] Rhea EM, Logsdon AF, Hansen KM, et al. The S1 protein of SARS-CoV-2 crosses the blood–brain barrier in mice. Nat Neurosci 2021;24:368–78. https://doi.org/10.1038/s41593-020-00771-8.
[21] Bi Z, Hong W, Que H, He C, Ren W, Yang J, Lu T, Chen L, Lu S, Peng X, Wei X. Inactivated SARS-CoV-2 induces acute respiratory distress syndrome in human ACE2-transgenic mice. Signal Transduct Target Ther 2021 Dec 24;6(1):439. https://doi.org/10.1038/s41392-021-00851-6. PMID: 34952899; PMCID: PMC8705082.
[22] Frank MG, Nguyen KH, Ball JB, Hopkins S, Kelley T, Baratta MV, Fleshner M, Maier SF. SARS-CoV-2 spike S1 subunit induces neuroinflammatory, microglial and behavioral sickness responses: Evidence of PAMP-like properties. Brain Behav Immun 2022 Feb;100:267–77. https://doi.org/10.1016/j.bbi.2021.12.007. Epub 2021 Dec 13. PMID: 34915155; PMCID: PMC8667429.
[23] Clough E, Inigo J, Chandra D, Chaves L, Reynolds JL, Aalinkeel R, Schwartz SA, Khmaladze A, Mahajan SD. Mitochondrial dynamics in SARS-COV2 spike protein treated human microglia: implications for neuro-COVID. J Neuroimmune Pharmacol 2021 Dec;16(4):770–84. https://doi.org/10.1007/s11481-021-10015-6. Epub 2021 Oct 2.
[24] Theoharides TC. Could SARS-CoV-2 spike protein be responsible for long-COVID syndrome? Mol Neurobiol 2022 Mar;59(3):1850–61. https://doi.org/10.1007/s12035-021-02696-0. Epub 2022 Jan 13. PMID: 35028901; PMCID: PMC8757925.
[25] Laubscher GJ, Lourens PJ, Steenkamp J, Kell DB, Pretorius E. SARS-CoV-2 spike protein S1 induces fibrin(ogen) resistant to fibrinolysis: implications for microclot formation in COVID-19. Biosci Rep 2021 Aug 27;41(8):BSR20210611. https://doi.org/10.1042/BSR20210611. PMID: 34328172; PMCID: PMC8380922.
[26] Poelzing S, Rosenbaum DS. Altered connexin43 expression produces arrhythmia substrate in heart failure. Am J Physiol Heart Circ Physiol 2004 Oct;287(4):H1762–70. https://doi.org/10.1152/ajpheart.00346.2004. Epub 2004 Jun 17 PMID: 15205174.
[27] Akar FG, Nass RD, Hahn S, Cingolani E, Shah M, Hesketh GG, DiSilvestre D, Tunin RS, Kass DA, Tomaselli GF. Dynamic changes in conduction velocity and gap junction properties during development of pacing-induced heart failure. Am J Physiol Heart Circ Physiol 2007 Aug;293(2):H1223–30. https://doi.org/10.1152/ajpheart.00079.2007. Epub 2007 Apr 13 PMID: 17434978.
[28] Akar FG, Tomaselli GF. Conduction abnormalities in nonischemic dilated cardiomyopathy: basic mechanisms and arrhythmic consequences. Trends Cardiovasc Med 2005 Oct;15(7):259–64. https://doi.org/10.1016/j.tcm.2005.08.002. PMID: 16226681.
[29] Radwański PB, Johnson CN, Györke S, Veeraraghavan R. Cardiac arrhythmias as manifestations of nanopathies: an emerging view. Front Physiol 2018 Sep;4(9):1228. https://doi.org/10.3389/fphys.2018.01228. PMID: 30233404; PMCID: PMC6131669.
[30] Veeraraghavan R, Gourdie RG, Poelzing S. Mechanisms of cardiac conduction: a history of revisions. Am J Physiol Heart Circ Physiol 2014 Mar 1;306(5):H619–27. https://doi.org/10.1152/ajpheart.00760.2013. Epub 2014 Jan 10. PMID: 24414064; PMCID: PMC3949060.
[31] Strauss RE, Mezache L, Veeraraghavan R, Gourdie RG. The Cx43 carboxyl-terminal mimetic peptide αCT1 protects endothelial barrier function in a ZO1 binding-competent manner. Biomolecules 2021 Aug 12;11(8):1192. https://doi.org/10.3390/biom11081192. PMID: 34439858; PMCID: PMC8393261.
[32] Mezache L, Struckman HL, Greer-Short A, Baine S, Györke S, Radwański PB, Hund TJ, Veeraraghavan R. Vascular endothelial growth factor promotes atrial arrhythmias by inducing acute intercalated disk remodeling. Sci Rep 2020 Nov 24;10(1):20463. https://doi.org/10.1038/s41598-020-77562-5. PMID: 33235263; PMCID: PMC7687901.